Cellular/Molecular

Axonal $GABA_A$ Receptors Increase Cerebellar Granule Cell Excitability and Synaptic Activity

Jason R. Pugh and Craig E. Jahr
Vollum Institute, Oregon Health & Science University, Portland, Oregon 97239

We report that activation of $GABA_A$ receptors on cerebellar granule cell axons modulates both transmitter release and the excitability of the axon and soma. Axonal $GABA_A$ receptors depolarize the axon, increasing its excitability and causing calcium influx at axonal varicosities. GABA-mediated subthreshold depolarizations in the axon spread electrotonically to the soma, promoting orthodromic action potential initiation. When chloride concentrations are unperturbed, GABA iontophoresis elicits spikes and increases excitability of parallel fibers, indicating that $GABA_A$ receptor-mediated responses are normally depolarizing. GABA release from molecular layer interneurons activates parallel fiber $GABA_A$ receptors, and this, in turn, increases release probability at synapses between parallel fibers and molecular layer interneurons. These results describe a positive feedback mechanism whereby transmission from granule cells to Purkinje cells and molecular layer interneurons will be strengthened during granule cell spike bursts evoked by sensory stimulation.

Introduction

In the traditional view, axonal signaling is limited to all-or-none action potentials that initiate near the soma and propagate orthodromically. This view of the axon has been challenged recently by evidence of analog signaling in the axon. Several groups have shown that subthreshold depolarizations of the soma can spread electrotonically several hundred micrometers out the axon and can result in increased vesicle release at synaptic terminals (Alle and Geiger, 2006; Shu et al., 2006; Kole et al., 2007; Christie and Jahr, 2008). Analog signaling need not be initiated at the soma; it can also be produced by activation of ligand-gated receptors expressed on the axon, which can also alter release probability and axonal excitability (Schmitz et al., 2001; Turecek and Trussell, 2001; Ruiz et al., 2003, 2010; Rusakov et al., 2005; Alle and Geiger, 2007). Furthermore, basic cable properties of unbranched axons suggests that subthreshold depolarizations initiated by ligand-gated receptors in the axon can spread electrotonically back toward the soma, possibly modulating action potential initiation at the axon initial segment (Paradiso and Wu, 2009).

$GABA_A$ receptor ($GABA_AR$) expression in particular has been observed or inferred in the presynaptic membranes of several synapses in the CNS (Eccles et al., 1963; Nicoll and Alger, 1979; Zhang and Jackson, 1993; Pouzat and Marty, 1999; Jang et al., 2001; Turecek and Trussell, 2002; Alle and Geiger, 2007). Unlike somatodendritic $GABA_A$Rs, these receptors generally produce depolarizing responses as a result of high chloride concentrations maintained in the axon (Zhang and Jackson, 1995; Price and Trussell, 2006). Activation of presynaptic $GABA_A$Rs has been shown to increase (Turecek and Trussell, 2002; Jang et al., 2006; Alle and Geiger, 2007) or decrease (Eccles et al., 1963; Zhang and Jackson, 1995) release probability depending on the synapse.

Recent evidence by Stell et al. (2007) suggests that $GABA_A$Rs are expressed on cerebellar granule cell axons and their activation increases evoked and spontaneous EPSCs recorded in Purkinje or stellate cells. However, as the mechanisms of $GABA_A$R-mediated modulation of EPSCs are not clear, we made direct recordings of $GABA_A$R activity in parallel fibers.

In this study, we find that activation of parallel fiber $GABA_A$Rs increases synaptic transmission by both increasing release probability at parallel fiber synapses and increasing the excitability of both the axon and soma/initial segment. $GABA_A$R activation increases axonal excitability and in some cases evokes antidromic spikes. This is true whether GABA is applied by iontophoresis or endogenous GABA release and spillover is evoked by activation of molecular layer interneurons (MLIs). Subthreshold depolarizations mediated by $GABA_A$Rs spread electrotonically back to the soma, increasing excitability of the soma/initial segment. Parallel fiber $GABA_A$Rs elicit calcium influx in axonal varicosities independent of spiking and increase release probability at individual parallel fiber synapses.

Materials and Methods

Slice preparation and electrophysiology. Acute parasagittal and horizontal brain slices were prepared from the cerebella of P14–P19 or P26–P28 Sprague Dawley rats, an age range well after the depolarizing/hyperpolarizing developmental switch in chloride reversal potential in other CNS regions (~P7) (Cherubini et al., 1991; Ehrlich et al., 1999; Stein et al., 2004) and after cerebellar granule cells have reached adult patterns of chloride transporter mRNA expression (<P14) (Mikawa et al., 2002). Rats were deeply anesthetized with isoflurane before removal of the cerebellum in accordance with Oregon Health & Science University institutional protocols and guidelines. The cerebellum was immediately placed in an ice-cold oxygenated solution containing the following (in mM): 110 choline chloride, 25 glucose, 25 $NaHO_3$, 11.5 sodium ascorbate, 7 $MgCl_2$, 3 sodium pyruvate, 2.5 KCl, 1.25 NaH_2PO_4, and 0.5 $CaCl_2$, and 300-μm-

Received Aug. 27, 2010; revised Oct. 18, 2010; accepted Oct. 31, 2010.

This work was supported by National Institutes of Health (NIH) Grant NS066037 and NIH Training Grant NS007381 (J.R.P.). We thank the Jahr laboratory members for discussions and critical readings of the manuscript.

Correspondence should be addressed to Craig E. Jahr, Vollum Institute L474, Oregon Health & Science University, 3181 SW Sam Jackson Park Road, Portland, OR 97239. E-mail: jahr@ohsu.edu.

DOI:10.1523/JNEUROSCI.4506-10.2011

 0270-6474/11/310565-10$15.00/0

thick slices were cut using a vibroslicer (Leica Instruments). The slices were incubated in warm (34°C) oxygenated artificial CSF (ACSF) solution containing the following (in mM): 119 NaCl, 26.2 $NaHO_3$, 2.5 KCl, 1 NaH_2PO_4, 1.3 $MgCl_2$, 2 $CaCl_2$, 11 glucose, for 30–60 min, after which they were incubated at room temperature. During recordings, slices were superfused with ACSF (22–24°C, except where noted) containing 10 μM NBQX (Ascent Scientific), 5 μM R-CPP (Ascent Scientific), and 1–5 μM CGP55845 (Tocris Bioscience) to isolate $GABA_A$-mediated currents, except where noted. Where indicated, solutions also contained 100 μM picrotoxin (Tocris Bioscience) or 200 nM TTX (Sigma).

Granule cells were identified with gradient contrast infrared optics (Dodt et al., 2002) and patched using borosilicate pipettes (4–6 MΩ) containing the following (in mM): 140 KCl, 4 $MgCl_2$, 10 HEPES, 4 Na-ATP, and 0.5 Na-GTP. Pipette solutions also contained the fluorescent dye Alexa 594 (50 μM) and the calcium-sensitive fluorescent dye Fluo-5F (200 μM) where indicated (Invitrogen). Electrophysiological currents and potentials were recorded with a Multiclamp 700B amplifier (Molecular Devices). Analog records were filtered at 5 kHz and digitized at 20–50 kHz. Data were collected using custom software (J. S. Diamond) written in IgorPro (Wavemetrics). GABA was locally applied through iontophoresis. An iontophoretic pipette (70–120 MΩ) containing 1 M GABA (pH 5) and 10 μM Alexa 594 was positioned near (<10 μm) the cellular process of interest, and GABA was ejected by a brief (5–50 ms) 50–200 nA current. A 4 nA backing current was maintained on the pipette to limit leak of GABA from the pipette in between GABA applications. Where possible, the effectiveness of GABA iontophoresis was tested on the soma or dendrites of the cell before and/or after iontophoresis on the axon. Parallel fibers were stimulated extracellularly by short voltage pulses (100 μs, 10–80 V) through a patch pipette filled with ACSF and 10 μM Alexa 594 placed in the molecular layer. During excitability testing the stimulus intensity was adjusted before each experiment to elicit action potentials in <50% of trials. As axons are very sensitive to small changes in stimulus intensities, a mixture of action potential successes and failures could only be elicited over a very narrow range of intensities. Therefore, the frequency with which action potentials were evoked often changed during the course of the experiment, likely due to small movements of the stimulating electrode or tissue. To maintain an action potential frequency below 50% without biasing the data, the stimulus intensity was only adjusted after a pair of trials (consisting of one control trial and one iontophoretic trial) and never in the middle of a pair.

Stellate cells were visually identified in the outer third of the molecular layer and patched with an internal solution containing the following (in mM): 144 K-gluconate, 4 $MgCl_2$, 10 HEPES, 4 Na-ATP, and 0.5 Na-GTP; where indicated by the text, 10–50 μM Alexa 594 and 200 μM Fluo-5F were also included. EPSCs were elicited by either parallel fiber stimulation in the molecular layer or granule cell layer stimulation. Ten to twenty micromolar muscimol (Tocris Bioscience) was applied using a Picospritzer (General Valve) though a borosilicate pipette positioned above the slice (3–9 psi). Minimal tissue movement was observed during puffing. In some cases, muscimol application decreased, rather than increased, EPSC amplitudes. In these cases, moving the pipette further from the slice generally produced an increase in EPSC amplitude, consistent with earlier reports that higher concentrations of muscimol decrease EPSC amplitudes (Stell and Marty, 2009), possibly due to inactivation of sodium or calcium channels in the axon. In some cases, the stimulus intensity was increased following bath application of EGTA-AM.

In experiments investigating changes in synaptic activity elicited by $GABA_A$R activation, a stimulating electrode was placed near the distal end of a stellate cell dendrite. NMDA receptor and $GABA_B$ receptor antagonists, R-CPP (5 μM) and CGP55845 (3–5 μM), were included in the bath solution during these experiments. Stimulus-evoked AMPA receptor-mediated calcium responses were often observed during axial line scans of the dendrites nearest the stimulating electrode, indicating the location of activated synapses. Release probability of the synapse was estimated by calculating the percentage of trials in which a calcium response was observed. Synaptic calcium responses were compared in control conditions and in the presence of GABA.

Bulk loading of parallel fiber tracts with fluorescent dyes was performed using either membrane-permeable AM-ester dyes (Regehr and Tank, 1991; Yuste and Konnerth, 2005) or dextran-conjugated dyes (Beierlein et al., 2004; Zhang and Linden, 2009). Horizontal cerebellar slices were placed in a recording chamber and perfused with ACSF at a relatively high flow rate (~4 ml/min). The tip of a patch pipette was broken, yielding a tip diameter of 20–30 μm, and filled with a fluorescent dye and fast green for visualization. In experiments using membrane-permeable dyes, 92 μM Oregon Green BAPTA-488 AM or 113 μM Magnesium Green AM (Invitrogen) were used. In experiments using dextran-conjugated dyes, the pipette was filled with a solution containing 0.04% Triton X-100, 0.17% dextran-conjugated Alexa 594 [10,000 molecular weight (MW); Invitrogen], and 1.7% dextran-conjugated fluo-4 (10,000 MW; Invitrogen). The tip of the pipette was positioned at the surface or a few micrometers within the molecular layer, and dye was ejected by applying a small positive pressure (0.02–0.2 psi). A second suction pipette was placed above the area of dye loading to remove excess dye. Fibers were loaded for 30–50 min (AM dyes) or 2–3 min (dextran-conjugated dyes) and then incubated for 1–2 h, allowing the dye to diffuse throughout the labeled parallel fibers. The density of loaded fibers decreased with distance from the loading zone, making it possible to find isolated labeled fibers 200–400 μm from the loading zone using two-photon laser-scanning microscopy (2PLSM).

2PLSM. Two-photon microscopy was performed on a custom two-photon laser-scanning microscope using an Olympus upright microscope and a Ti:sapphire laser (Coherent) tuned to 810 nm. Photomultipliers (H8224, Hamamatsu) collected red and green light in both the epifluorescence and transfluorescence pathways (Christie and Jahr, 2008). ScanImage software (Pologruto et al., 2003) was used for acquisition. Line scans were performed at 500 Hz. Fluorescence changes were calculated by subtracting the baseline from the green trace and dividing by the red trace ($\Delta G/R$), or in cases where a red dye was not used, subtracting and dividing by the baseline fluorescent signal ($\Delta F/F$).

Analysis. Data were analyzed using IgorPro (Wavemetrics), ImageJ (NIH), and AxoGraph (AxoGraph Scientific) software. Statistical significance was determined using paired Student's *t* tests in Excel (Microsoft). A value of $p \leq 0.05$ was considered significant. Data are reported as mean ± SE. Stimulus artifacts were digitally reduced in membrane current/voltage traces.

Results

$GABA_A$ receptor activation increases EPSC amplitudes

Whole-cell patch-clamp recordings were made from stellate cells in acute horizontal cerebellar slices, and pairs of EPSCs (20 ms interval) were evoked by molecular layer stimulation of parallel fibers. To test for effects of parallel fiber $GABA_A$R activation, muscimol (10–20 μM), a $GABA_A$R agonist, was applied by pressure onto the molecular layer. Muscimol increased EPSC amplitudes (Fig. 1*A*,*B*,*F*) (107 ± 20 pA vs 198 ± 32 pA, $p = 0.009$, $n = 7$), as has been previously reported (Stell et al., 2007), and decreased the paired-pulse ratio (PPR) (Fig. 1*B*,*F*) (2.04 ± 0.25 vs 1.6 ± 0.14, $p = 0.03$), suggesting that release probability was increased. We measured calcium transients in single parallel fiber varicosities during activation of $GABA_A$Rs using Fluo-5F, which was loaded through the patch pipette. Iontophoretic application of GABA produced a small calcium rise ($\Delta G/R$ 0.0054 ± 0.002, $n = 5$, $p = 0.048$) (Fig. 1*C*) in axonal varicosities in the presence of 200 nM TTX and 5 μM CGP55845, Na^+ channel and $GABA_B$ receptor antagonists, respectively. These findings suggest that $GABA_A$R activation increases release probability at parallel fiber synapses by depolarizing the axon and activating voltage-gated calcium channels.

As $GABA_A$Rs are depolarizing in these conditions, it is possible that their activation increases EPSC amplitudes by increasing parallel fiber excitability in addition to increasing release probability. To distinguish between these mechanisms, the membrane-permeable calcium chelator, EGTA-AM (20 μM), was added to

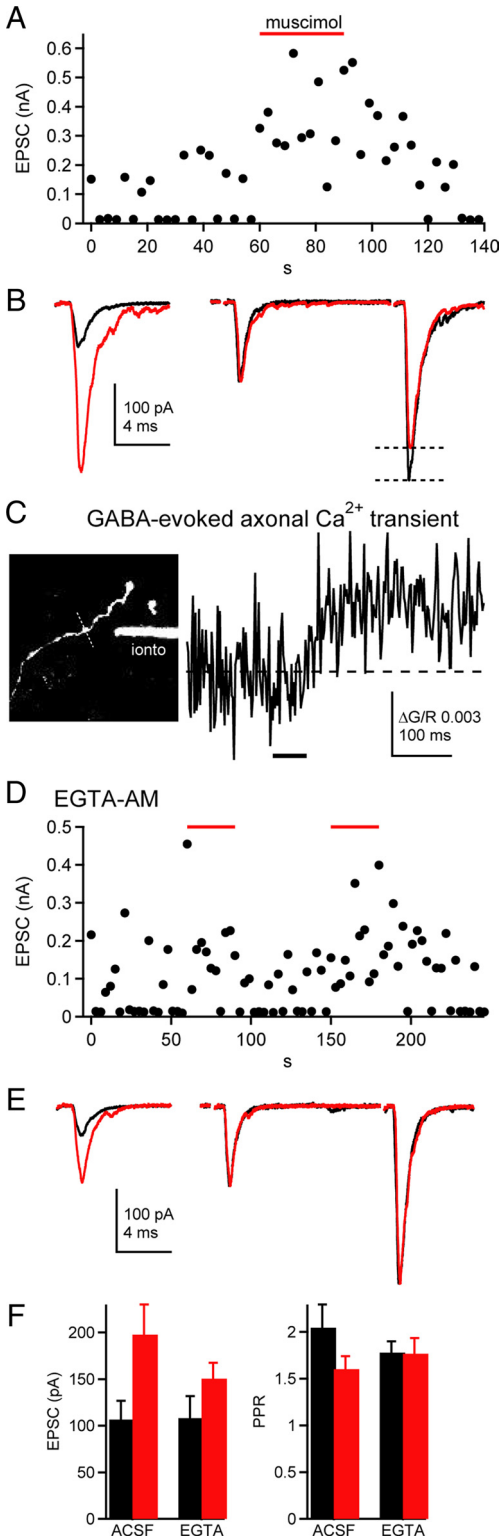

Figure 1. Muscimol increases release probability and parallel fiber excitability. ***A***, EPSC amplitudes recorded from a stellate cell. EPSCs were elicited by molecular layer stimulation. Red bar indicates timing of muscimol (20 μM) application. ***B***, Average EPSC (left) or pair of EPSCs normalized to the first response (right) in control (black) or in the presence of muscimol (red). ***C***, Left, Image of a granule cell axon and iontophoretic pipette. Right, Representative $\Delta G/R$ transient following GABA iontophoresis (thick bar) in the presence of 200 nM TTX. ***D***, EPSC amplitudes recorded from the same cell as in ***A*** in the presence of EGTA-AM (20 μM). ***E***, Average EPSC (left) or pair of EPSCs normalized to the first response (right) in control (black) or in the presence of muscimol (red). ***F***, Average EPSC amplitudes and paired-pulse ratios in control (black) or muscimol (red).

the superfusate to block the rise in intracellular calcium and release probability following $GABA_AR$ activation. Subsequent application of muscimol still increased EPSC amplitudes (Fig. 1*D–F*) (108 ± 24 vs 151 ± 17 pA, $p = 0.01$, $n = 6$), though not to the extent observed in control ACSF. However, unlike in control conditions, the PPR was unchanged by muscimol in the presence of EGTA-AM (Fig. 1*E,F*) (1.78 ± 12 vs 1.76 ± 17, $p = 0.91$), indicating no change in release probability. These data suggest that $GABA_AR$ activation in parallel fibers has at least two effects, increasing excitability of parallel fibers and increasing release probability at parallel fiber to stellate cell synapses.

$GABA_AR$-mediated depolarizations increase axonal excitability

To explicitly test the effects of axonal $GABA_AR$ activation on parallel fiber excitability, we used the method of excitability testing (Kocsis et al., 1983; Christie and Jahr, 2009). Single parallel fibers were visualized by filling granule cells with Alexa Fluor-594 through the patch pipette. The axon could then be followed out to the molecular layer beyond the parallel fiber branch point, in some cases for hundreds of micrometers. To isolate $GABA_AR$-mediated currents, CPP (5 μM), NBQX (10 μM), and CGP55845 (1–5 μM) were included in the bath. Action potentials were evoked in the labeled axon by brief (100–200 μs) current pulses delivered through a stimulating pipette adjacent to the labeled axon (Fig. 2*A*). Axonal stimulation produced rapidly rising (<1 ms), but relatively small (5–20 mV) depolarizations at the soma rather than full amplitude spikes (Fig. 2*B*, red trace), probably due to the failure of antidromic spikes to fully invade the somatic compartment (Coombs et al., 1957; Fuortes et al., 1957; Kandel et al., 1961; Scobey and Gabor, 1975). To confirm that these relatively small somatic depolarizations are full spikes in the axon, we recorded calcium transients in axonal varicosities elicited by orthodromic and antidromic spikes and found no difference in calcium response amplitudes (Fig. 2*B*) ($\Delta G/R$ 0.057 ± 0.012 vs 0.055 ± 0.012, $p = 0.34$, $n = 9$). This was true whether calcium signals were measured in the ascending axon ($n = 5$), in the stimulated parallel fiber ($n = 4$) or in the unstimulated parallel fiber branch ($n = 5$).

Despite the supralinear nature of action potential initiation, there is a very narrow range of stimulus intensities over which a mixture of successes and failures can be elicited by axonal stimulation (Fig. 2*D*) (Paradiso and Wu, 2009). By fine tuning the stimulus intensity, we were able to elicit axonal action potentials, detected as broken spikes in the soma, on <50% of the trials (Fig. 2*C*, left). On alternating trials, GABA was briefly (5–30 ms) iontophoresed onto the axon near the stimulating electrode 50–100 ms preceding the stimulus. Axonal excitability was assessed by measuring the spike probability in each condition. On trials in which GABA was iontophoresed, the electrical stimulation of the axon was more likely to produce a spike, increasing the success rate from 40.9 ± 6% to 72.6 ± 8 (Fig. 2*C,E*) ($p = 0.01$, $n = 6$).

In some cases, iontophoresis alone produced broken spikes at the soma indistinguishable in time course and amplitude from spikes evoked by electrical stimulation of the axon (Fig. 2*F,G*) (10–90% rise time: 0.9 ± 0.06 ms, $n = 10$ vs 0.8 ± 0.04 ms, $n = 7$, $p = 0.22$; amplitude at −70 mV: 8.4 ± 1.12 mV, $n = 9$, vs 8.96 ± 1.66 mV, $n = 6$, $p = 0.92$). These data demonstrate that activation of $GABA_ARs$ increases excitability of parallel fibers, in some cases bringing fibers to action potential threshold.

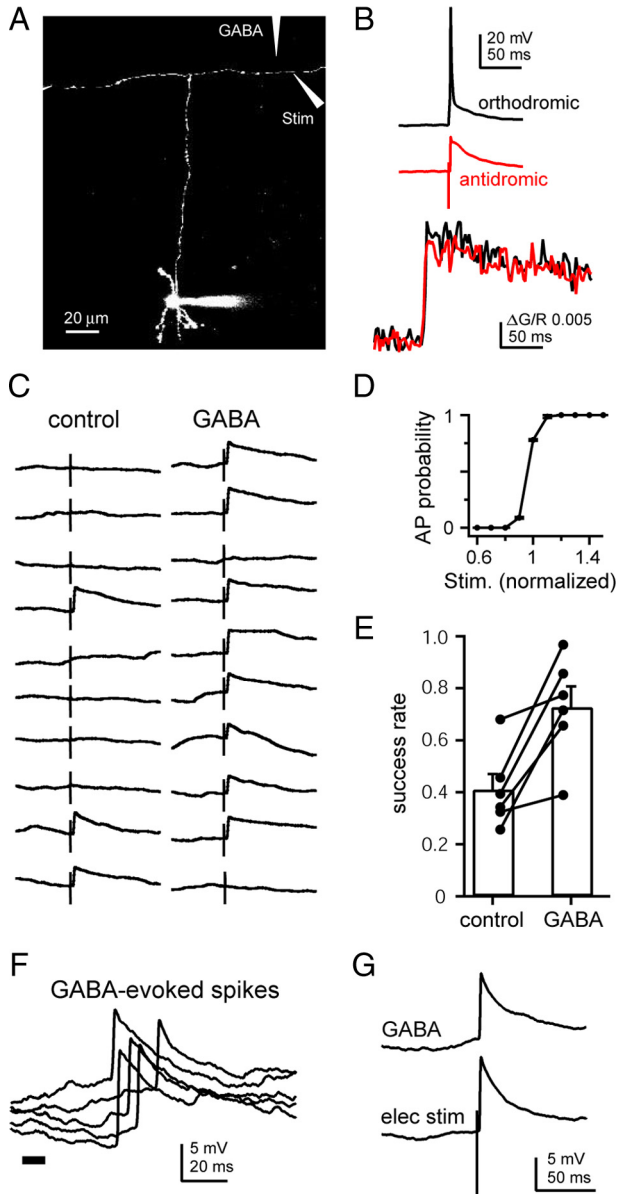

Figure 2. GABA iontophoresis on the axon increases axon excitability and elicits antidromic spikes. ***A***, Maximal projection image of a cerebellar granule cell filled with Alexa 594. The ascending axon, branch point, and parallel fibers are visible. Stimulating and iontophoretic pipettes were added digitally to demonstrate the experimental setup. ***B***, Voltage traces recorded at the soma (top) and calcium responses recorded from the axon (bottom) of orthodromic (black traces) or antidromic (red traces) action potentials. ***C***, Ten pairs of consecutive alternating voltage traces showing single axonal stimuli either in control conditions (left) or following iontophoresis of GABA on the axon (right). ***D***, Average action potential probability plotted against the intensity of axonal stimulation. Stimulus intensity was normalized to the lowest value that produced spikes >50% of the time. ***E***, Average (bars) and individual cell (connected circles) spike success rates in control conditions and following GABA iontophoresis. ***F***, Representative examples of antidromic spikes recorded in the soma following GABA iontophoresis on the axon (thick bar). ***G***, Examples of antidromic spikes elicited by GABA iontophoresis (top) or electrical stimulation (bottom) in the same cell.

$GABA_A$Rs on parallel fibers are activated by endogenous release of GABA

The experiments above show that activation of axonal $GABA_A$Rs by exogenous GABA application increases excitability, but do not address whether endogenous GABA also activates axonal receptors. It has been shown previously that spillover of GABA from inhibitory synapses in the molecular layer can activate $GABA_B$ receptors at parallel fiber synapses onto Purkinje cells (Dittman and Regehr, 1997) and that enhancement of EPSCs in Purkinje cells by molecular layer stimulation can be blocked by gabazine (Stell et al., 2007), raising the possibility that parallel fiber $GABA_A$Rs are activated by spillover of GABA. We tested this possibility using excitability testing of parallel fibers. Granule cells were patched with an internal solution containing Alexa 594 and Fluo-5F. A stimulating electrode (S1) was positioned near the axon and the intensity adjusted such that action potentials were elicited <50% of the time. A second stimulating electrode (S2) was placed in the molecular layer to activate multiple MLIs either directly or through activation of parallel fibers (glutamate receptor antagonists were not present in these experiments) (Fig. 3*A*). S2 was placed at least 20 μm away from the labeled axon to avoid direct activation of the labeled axon. In alternating trials, a 100 Hz train of 10 stimuli was delivered through S2 beginning 100 ms before stimulating the labeled axon, a stimulus protocol previously shown to activate MLIs and cause spillover of GABA (Dittman and Regehr, 1997) and not substantially different from granule cell firing patterns observed *in vivo* (Chadderton et al., 2004). To prevent subthreshold voltage changes in the soma resulting from dendritic synaptic inputs from altering axonal excitability (Alle and Geiger, 2006; Shu et al., 2006; Kole et al., 2007; Christie and Jahr, 2009), the soma was voltage clamped at −60 mV. Despite the voltage clamp at the soma, action potentials were evoked in the axon by S1 and detected by the presence of both all-or-none calcium responses in the axon and action currents recorded at the soma (Fig. 3*B*,*C*). In all trials, calcium responses in the axon coincided with an action current at the soma. Compared to control trials, molecular layer stimulation increased action potential success rate by ~60% (34.8 ± 2.7% vs 55.6 ± 2.9%, $n = 5$, $p = 0.006$) (Fig. 3*C*,*D*). Picrotoxin abolished the change in excitability (46.9 ± 2.2 vs 47.2 ± 4.2, $n = 5$, $p = 0.93$) (Fig. 3*D*), confirming that the excitability change resulted from GABA release and not direct stimulation of the labeled axon by S2. Molecular layer stimulation increased spike probability without changing the average calcium response (Fig. 3*E*) ($\Delta G/R$ 0.049 ± 0.011 vs 0.051 ± 0.012) or action current amplitudes (10.1 ± 3.3 vs 11.5 ± 4.3 pA) evoked by individual action potentials. As direct axoaxonic synapses onto parallel fiber axons have not been observed (Palay and Chan-Palay, 1974), these data suggest that GABA released from inhibitory synapses in the molecular layer can diffuse from the site of release to nearby parallel fibers, activating axonal $GABA_A$Rs.

Chloride equilibrium potential in the intact axon

In the experiments presented so far, $GABA_A$R-mediated responses were depolarizing, as expected for the use of an internal recording solution containing a high chloride concentration. The endogenous chloride concentration in granule cell axons is unknown, though high chloride concentrations, as have been observed at other axon terminals (Zhang and Jackson, 1995; Price and Trussell, 2006), are expected (Fig. 1*F*) (Stell et al., 2007). To directly assess whether $GABA_A$R activation in the axon is excitatory, inhibitory, or shunting when the native chloride concentration is intact, we loaded parallel fibers with dextran-conjugated fluorescent dyes, Alexa 594 and Fluo-4. During loading, dye is trapped in parallel fiber axons and diffuses through their cytoplasm, creating a beam of loaded axons extending from the loading zone. Using 2PLSM, we imaged isolated single fibers 200–400 μm from the loading zone, where the density of loaded fibers is reduced (Fig. 4*A*). Because chloride concentrations are often developmentally regulated (Cherubini et al., 1991; Ehrlich et al.,

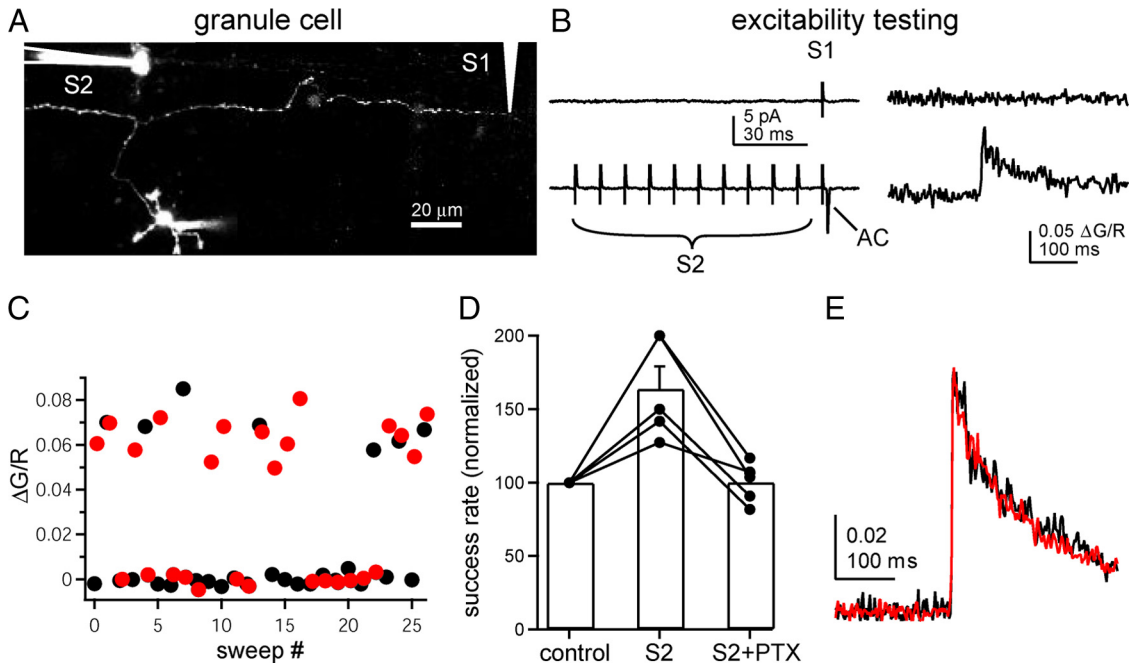

Figure 3. Spillover of endogenous GABA activates axonal $GABA_A$Rs. ***A***, Image of a granule cell filled with Alexa-594 and Fluo-5F. The patch electrode (bottom), S1 stimulating electrode (right), and S2 stimulating electrode (left) are visible. Stimulating electrodes have been digitally enhanced for clarity. ***B***, Somatic current (left) and axonal fluorescence (right) traces of S1 stimulation alone (no action potential elicited; upper traces) or S1 stimulation proceeded by 10 stimuli at 100 Hz through S2 (lower traces; AC, action current). ***C***, Peak fluorescence following S1 stimulation alone (black circles) or with S2 stimulation (red circles) in 54 alternating trails. ***D***, Average (bars) and individual cell (connected circles) spike success rates (normalized to control) in control, with 100 Hz S2 stimulation, and with 100 Hz S2 stimulation in the presence of 100 μM picrotoxin. ***E***, Average calcium response of successes in control conditions (black trace) and following S2 stimulation (red trace).

1999; Stein et al., 2004) and chloride transporters may be effected by temperature, these experiments were performed in older animals (P26–P28) and at elevated temperature (33–36°C). Electrical stimulation of individual labeled fibers elicited all-or-none calcium signals in axonal varicosities 5–20 μm from the site of stimulation (Fig. 4*A*,*B*). Using this calcium response as an indicator of an action potential in the labeled axon, we assessed the excitability of the axon with and without GABA iontophoresis. In control trials, a minimal electrical stimulus produced an action potential 40.3 ± 2.7% of the time, while in interleaved trials in which electrical stimulation was preceded by GABA iontophoresis, action potentials were generated 61.8 ± 4.1% of the time (Fig. 4*B*,*D*) ($n = 11, p < 0.001$). Because success and failure trials were sorted visually, it is possible that some action potential-evoked calcium responses were too small to be distinguished from the noise or that noise was mistaken for an evoked calcium response in some cases. To address this, we first averaged all trials together, both successes and failures, for each condition and compared the average calcium responses. With no sorting of trials, the average calcium signal when GABA was iontophoresed was significantly larger than control (Fig. 4*C*, top) ($\Delta G/R$ 0.0089 ± 0.0014 vs 0.0052 ± 0.0007, $p = 0.003$; $n = 11$). When only the success trials in each condition were averaged, there was no difference in amplitude between control and GABA ($p = 0.23$), and averaging only the failure trials resulted in no detectable response in either condition ($\Delta G/R$ 0.00047 ± 0.0003), indicating the accurate sorting of successes and failures (Fig. 4*D*, bottom). Similar results were obtained by bulk loading parallel fibers from younger animals (P14–P19) with Oregon Green BAPTA488-AM and recording at room temperature (data not shown). The observation that GABA increases the excitability of the axon indicates that $GABA_A$Rs are depolarizing when the intracellular chloride concentration is unperturbed.

In slices prepared from juvenile animals, some axons filled with Oregon Green BAPTA1-AM exhibited picrotoxin-sensitive all-or-none calcium responses following GABA iontophoresis alone ($n = 7$). These responses were also probably the result of action potential-evoked calcium influx, as they were similar in amplitude and time course to responses produced by direct electrical stimulation of the axon (Fig. 4*E*,*F*) (electrical stimulation: $\Delta F/F$ 0.35 ± 0.05%, $n = 9$; GABA stimulation: 0.38 ± 0.08%, $n = 7$, $p = 0.73$). $GABA_A$R activation not only increased axon excitability, it was sufficient to initiate action potentials in the axon, indicating that the chloride equilibrium potential in these axons is near if not beyond spike threshold.

Axonal depolarization increases somatic excitability

In most cells patched with a high chloride internal solution, iontophoresis of GABA onto the labeled parallel fiber (Fig. 5*A*) (177 ± 15 μm from the soma) produced small (4.9 ± 0.8 mV, $n = 22$) and relatively slow (time to peak = 197 ± 13 ms) depolarizations recorded at the soma. These somatic depolarizations were blocked by bath application of 100 μM picrotoxin (Fig. 5*B*) (0.1 ± 0.5 mV, $n = 3$) or by moving the iontophoretic pipette 20–30 μm away from the axon (Fig. 5*C*) (0.14 ± 0.42 mV; $n = 6$), confirming that axonal, and not somatic, $GABA_A$Rs mediated the depolarizations. This raises the possibility that in addition to locally increasing the excitability of the axon, subthreshold $GABA_A$R-mediated depolarizations can also electrotonically spread through the axon for hundreds of micrometers (Alle and Geiger, 2006; Shu et al., 2006; Christie and Jahr, 2009) and alter spike initiation at the soma/axon initial segment.

To test this possibility, we first repeated the experiment in Figure 1 using stimulation of the granule cell layer (GCL) to evoke orthodromic action potentials instead of molecular layer stimulation, which activates parallel fibers directly. EPSCs recorded in stellate cells evoked by GCL stimulation were also enhanced by puffing muscimol onto the molecular layer (Fig. 6*A*) (151 ± 19% of control, $n = 6$, $p = 0.02$). This effect was

only partially blocked by bath application of EGTA-AM (130 ± 12% increase, $p = 0.057$), suggesting that more granule cells are brought to threshold by the stimulus when parallel fiber $GABA_A$Rs are activated.

To measure the effects of axonal $GABA_A$R activation on somatic excitability more directly, action potentials were evoked in granule cell by current injection through the patch pipette. These somatic depolarizations were adjusted so that action potentials were elicited in <50% of trials and were paired, on alternate trials, with axonal GABA iontophoresis in the molecular layer, 132 ± 26 μm from the soma. GABA iontophoresis increased spike probability from 0.27 ± 0.04 in control to 0.71 ± 0.06 (Fig. 6*B*,*C*) ($n = 7$, $p = 0.002$). The increase in spike probability was correlated with the amplitude of depolarization in the soma following GABA iontophoresis alone ($r^2 = 0.54$). These results indicate that depolarizations arising in distant regions of the axon are integrated, presumably by the initial segment, with somatodendritic potentials to produce spikes.

$GABA_A$R activation increases synaptic response probability

As suggested by the effects on PPR (Fig. 1), activation of parallel fiber $GABA_A$Rs also increases release probability at parallel fiber synapses. However, to assess more directly the effects of axonal $GABA_A$Rs on release probability, it is necessary to measure changes in release independently of changes in axonal or somatic excitability. This was accomplished by performing optical quantal analysis (Oertner et al., 2002) of single parallel fiber synapses onto MLIs. MLIs were filled through the patch pipette with Alexa 594 and Fluo-5F. Parallel fiber input was evoked with a stimulating electrode positioned near a MLI dendrite (Fig. 7*A*). Sites of synaptic activation were detected with line scans running axially through dendrites near the stimulating electrode (Fig. 7*B*). With NMDA receptors blocked, stimulation of parallel fibers evoked calcium transients mediated by calcium-permeable AMPA receptors (Soler-Llavina and Sabatini, 2006; Kelly et al., 2009). To confirm that calcium signals represented the activation of a single synapse, the spatial distribution of the peak signal was fitted with a Gaussian (Fig. 7*C*). The width of the calcium response, as measured by the standard deviation of the Gaussian, was 0.75 ± 0.04 μm ($n = 8$), in close agreement with previous estimates of the spatial extent of calcium from single synapses in MLIs (Soler-Llavina and Sabatini, 2006) and in fast spiking cortical interneurons (Goldberg et al., 2003). Once a synaptic calcium response was located, an iontophoretic pipette was positioned near the dendrite, and GABA was ejected on alternating trials of parallel fiber stimulation. Averaging across all trials, iontophoresis of GABA increased the postsynaptic calcium response by 40% compared to control trials (Fig. 7*D*,*E*) ($\Delta G/R$ 0.0074 ± 0.002 vs 0.01 ± 0.002, $n = 13$, $p = 0.02$). Increased release probability may change the average calcium response by decreasing the number of failures and/or increasing the number of vesicles released. Multivesicular release has been observed at this synapse and is proportional to release probability (Foster et al., 2005; Bender et al., 2009), raising the possibility that single response amplitudes can be increased. We

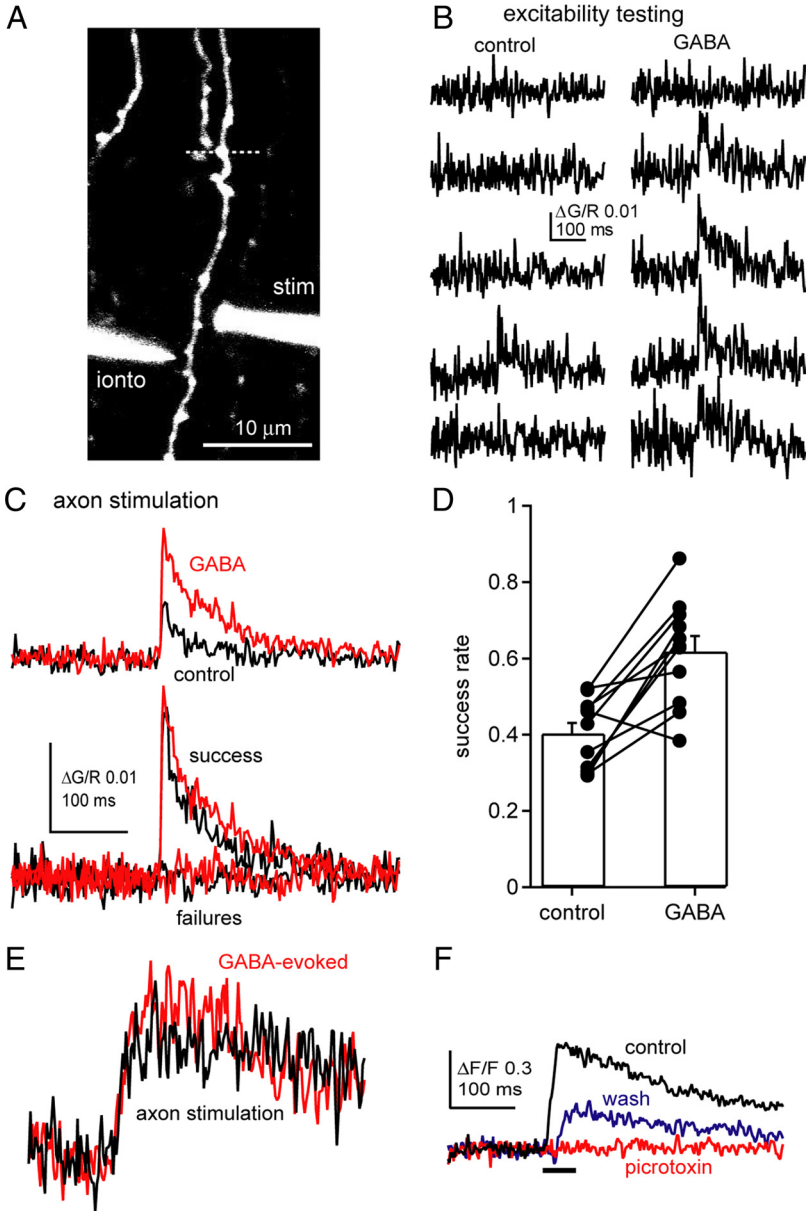

Figure 4. GABA-mediated responses are excitatory when axonal chloride is unperturbed. ***A***, Image of a single parallel fiber loaded with dextran-conjugated Alexa 594 and Fluo-4. The stimulating pipette and iontophoretic pipette are also visible. The line scan location is also shown (dashed line). ***B***, Five pairs of consecutive alternating calcium-dependent fluorescent traces during single axonal stimuli either in control conditions (left) or following GABA iontophoresis (right) from the axon shown in ***A***. ***C***, Top, Calcium responses averaged across all trials in control (black) or following GABA iontophoresis (red). Bottom, Average of successes (upper traces) and failures (lower traces) in control conditions (black) and following GABA iontophoresis (red). ***D***, Average (bars) and individual cell (connected circles) spike success rates in control conditions and following GABA iontophoresis. ***E***, Calcium responses elicited by either electrical stimulation (black) or GABA iontophoresis (red) in the same axon. ***F***, Average calcium responses elicited by GABA iontophoresis before (black), during (red), and following (blue) bath application of 100 μM picrotoxin. Traces in ***E*** and ***F*** are at the same scale.

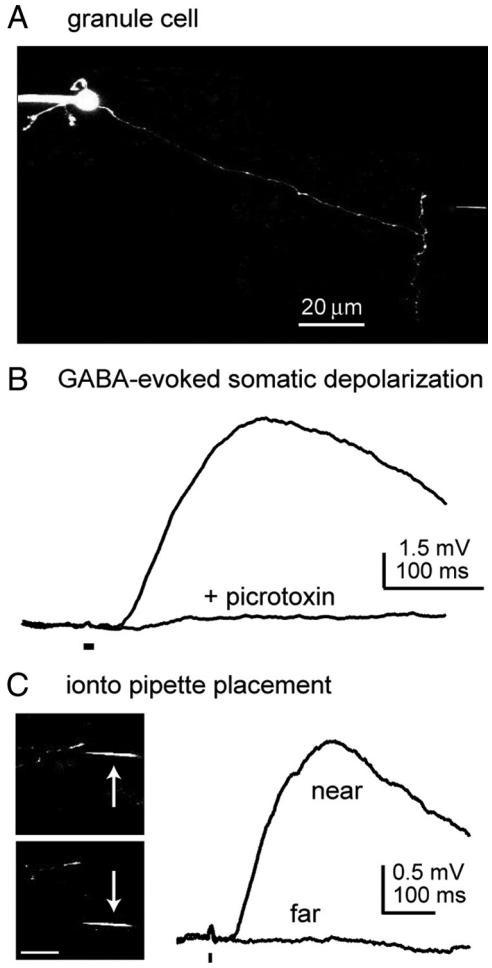

Figure 5. GABA iontophoresis on the axon produces somatic depolarization. ***A***, Image of a cerebellar granule cell filled with Alexa-594. The iontophoretic pipette can be seen at the right. ***B***, Representative depolarization recorded in the soma following GABA iontophoresis on the axon (thick bar) in control ACSF (upper trace) and in the presence of picrotoxin (lower trace). ***C***, Images of a labeled parallel fiber and iontophoretic pipette (left) and voltage responses recorded at the soma (right) when the iontophoretic pipette is positioned adjacent to the axon (upper image/trace) or 21.6 μm from the axon (lower image/trace). Scale bar, 10 μm.

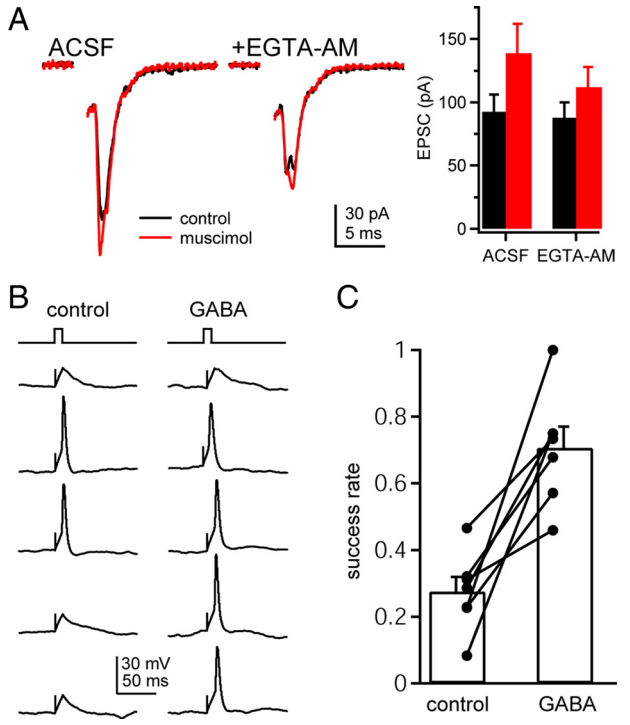

Figure 6. Axonal $GABA_A$Rs increase somatic excitability. ***A***, Representative EPSC (left) and average EPSC amplitudes (right) before/after (black) or during (red) muscimol application in control ACSF or in the presence of EGTA-AM (20 μM). EPSC were evoked by a bipolar electrode placed in the granule cell layer and recorded in stellate cells. ***B***, Voltage traces from 5 pairs of granule cell somatic depolarization in control conditions (left) or proceeded by GABA iontophoresis on the axon (right). ***C***, Average (bars) and individual cell (connected circles) spike success rates in control conditions and following GABA iontophoresis.

distinguished between these two possibilities by visually sorting trials as successes or failures. In the averages of failures, calcium responses were not detected or were exceedingly small ($\Delta G/R$ 0.0017 ± 0.0005), suggesting that responses in individual trials were large enough to be visually identified and confirming that trials were sorted accurately. The amplitude of calcium responses in successful trails was the same for control and GABA trials ($\Delta G/R$ 0.02 ± 0.004 vs 0.02 ± 0.004), indicating that response amplitude is not changed by GABA (Fig. 7*D*, bottom, *E*). We did observe an increase in response amplitude during paired-pulse stimuli. The amplitude of the calcium response to the first stimulus was smaller than responses to the second stimulus when there was a failure on the first ($\Delta G/R$ 0.019 ± 0.0047 vs 0.036 ± 0.008, $p = 0.007$, $n = 10$) (Fig. 7*F*), indicating that more glutamate is released on the second stimulus, most likely through increased multivesicular release, and that postsynaptic AMPA receptors are not saturated by a single stimulus.

To directly assess changes in release probability, we calculated the percentage of successful trials in control and following GABA iontophoresis. Release probability was increased by GABA iontophoresis in 12 of 13 synapses tested (Fig. 7*G*) (control, 0.38 ± 0.07; GABA, 0.54 ± 0.07, $p < 0.001$). However, an increase in successful trials may result from an enhanced excitability of the axon rather than a true increase in the probability of vesicular release. Given the sharp threshold of action potential initiation (Fig. 2*C*) (Paradiso and Wu, 2009), it is likely that spike probability of the axon was at or near 1 with the stimulus intensities used in these experiments. However, to rule out the possibility that GABA increased spike probability, we bath-applied the membrane-permeable calcium chelator, EGTA-AM. EGTA is expected to reduce presynaptic calcium, and thus release probability, but not to change axonal excitability elicited by GABA. In contrast to the effects of EGTA-AM on EPSC amplitudes (Figs. 1*F*, 6*A*), the increase in response probability evoked by GABA was blocked by EGTA-AM (Fig. 7*G*) (control 212 ± 53%, EGTA-AM 99 ± 8%, $n = 6$, $p = 0.02$). This suggests that postsynaptic calcium responses arise from a single activated synapse and the increased response probability reflects an increased release probability at that synapse, not excitation of additional nearby synapses or increased reliability of axonal stimulation.

Discussion

We find that $GABA_A$R activation in cerebellar parallel fibers results in subthreshold and suprathreshold depolarizations, increased axonal excitability, and increased release probability at synapses onto stellate interneurons. $GABA_A$R-mediated responses are excitatory when internal ion concentrations are intact and can be activated by spillover of endogenously released GABA, consistent with earlier findings (Stell et al., 2007). We also find that subthreshold depolarizations generated by axonal

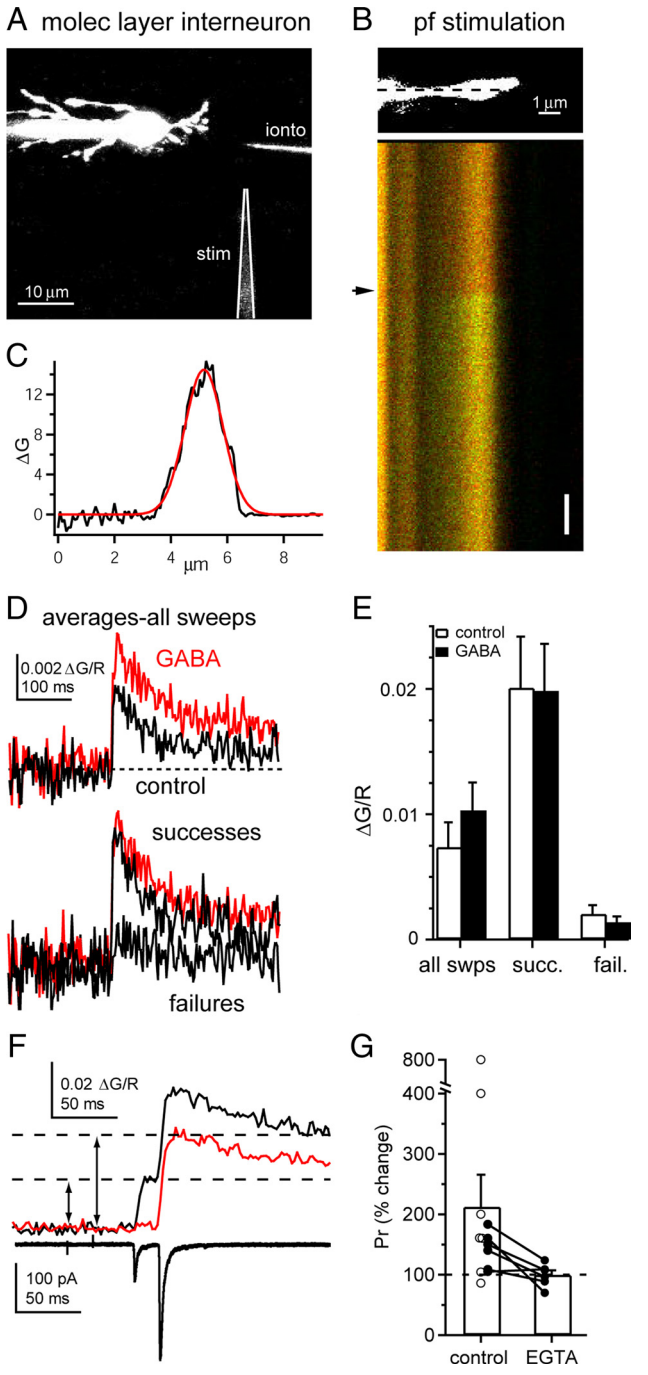

Figure 7. GABA increases release probability at parallel fiber stellate cell synapses. ***A***, Top, Image of a stellate cell filled with Alexa-594 and Fluo-5F. The stimulating pipette and iontophoretic pipette are also visible (digitally enhanced for clarity). ***B***, Magnified image of a single dendrite (top) and line scan across the long axis of the dendrite at 500 Hz showing red and green (calcium dependent) fluorescence (bottom). Arrow indicates the time of parallel fiber stimulation. Calibration: 50 ms. ***C***, Average spatial distribution of the peak green fluorescence in the synapse shown in ***B*** from the first 10 ms following stimulation. The fluorescence profile is fit with a Gaussian curve (red). ***D***, Top, Average postsynaptic calcium responses of all trials in control conditions (black) and following GABA iontophoresis (red). Bottom, Average of success trials only (upper traces) or failure trials only (lower trace). ***E***, Average peak calcium responses across all cells when all trials, successes only, or failures only are average. ***F***, Top, The average postsynaptic calcium response following paired-pulse parallel fiber stimulation when there is a success on the first stimulus (black) or a success on the second stimulus following a failure on the first (red). Bottom, Average of all EPSCs from the same cell. ***G***, Average (bars) and individual cell (circles) changes in response probability due to GABA iontophoresis in control conditions or EGTA. Data taken from the same cells are connected by lines.

$GABA_A$Rs can spread electrotonically back to the soma, where they increase the excitability of the soma/axon initial segment.

Axons maintain high chloride concentrations

Axonal $GABA_A$Rs have been detected in a number of neurons throughout the nervous system (Eccles et al., 1963; Zhang and Jackson, 1993; Pouzat and Marty, 1999; Turecek and Trussell, 2002; Ruiz et al., 2003, 2010; Szabadics et al., 2006; Alle and Geiger, 2007; Christie and Jahr, 2009). Unlike somatodendritic $GABA_A$Rs, which are generally hyperpolarizing, axonal $GABA_A$Rs are often depolarizing (Eccles et al., 1963; Jang et al., 2001; Turecek and Trussell, 2002), indicating that large chloride gradients can be maintained between compartments (Price and Trussell, 2006; Szabadics et al., 2006), allowing high chloride concentrations in axons. Where E_{Cl} has been measured in axons, it has been found to be near −50 mV, depolarized from rest, but not beyond action potential threshold (Zhang and Jackson, 1995, Price and Trussell, 2006).

Intracellular chloride concentration is determined by the balance of chloride extrusion, mediated by the potassium-dependent chloride transporters KCC1 and KCC2 in neurons, and chloride accumulation, mediated by the sodium and potassium-dependent transporters NKCC1 and NKCC2. High chloride concentrations are generally associated with reduced KCC2 expression, as is seen in many neuron types early in development (Stein et al., 2004), and increased NKCC1 and 2 expression (Yamada et al., 2004; Sipilä et al., 2009). In the adult cerebellum, KCC2 mRNA is expressed throughout the cortex, while NKCC1 mRNA is only expressed in granule cells (Kanaka et al., 2001; Mikawa et al., 2002), consistent with the maintenance of high chloride concentrations in the axons of these cells. Chloride transporters can be modulated by phosphorylation (Flatman, 2002; Rinehart et al., 2009). The extent to which this is altered in acute brain slices is not known.

Effects on synaptic release probability

Even when the chloride reversal potential in the presynaptic terminal is depolarized relative to the resting membrane potential, $GABA_A$R activation does not necessarily increase synaptic activity. $GABA_A$R-mediated depolarizations can influence release in a number of ways. In some cases, depolarization activates voltage-gated calcium channels, increasing release through calcium influx at the bouton (Turecek and Trussell, 2001; Awatramani et al., 2005; Xiao et al., 2007). However, with larger or prolonged depolarization, calcium and sodium channels can become inactivated, inhibiting release (Ruiz et al., 2003; Awatramani et al., 2005; Jang et al., 2005; Stell and Marty, 2009). Electrotonic spread of subthreshold somatic depolarizations out the axon can inactivate potassium channels, broadening action potentials and increasing release (Kole et al., 2007). Subthreshold depolarizations initiated in the axon may also increase release by the same mechanism. Scott et al. (2008) have suggested that axonal depolarization alone, not accompanied by calcium influx, is sufficient to increase release. If so, the same mechanism may increase release during $GABA_A$R-mediated depolarization of the terminal. At parallel fiber synapses, it is likely that release probability is increased by $GABA_A$Rs due to calcium influx through voltage-gated calcium channels given that EGTA-AM blocks the effects of GABA on release probability and that GABA iontophoresis on the axon produces calcium increases in varicosities.

It is also possible that $GABA_A$R-mediated currents depolarize the axon sufficiently to initiate action potentials in the axon. This has been observed by Szabadics et al. (2006) in cortical pyramidal

cells due to direct axoaxonic synapses and in parallel fibers during GABA application (Stell et al., 2007). However, in the present study, this phenomenon was only observed during exogenous GABA application and not by spillover of endogenous GABA release.

Multivesicular release

The extent of MVR at parallel fiber to stellate cell synapses is directly related to the release probability of the synapse (Bender et al., 2009). However, we find that release probability was increased by presynaptic $GABA_A$R activation with no detectable changes in the postsynaptic calcium transient amplitude. Unlike reports of parallel fiber–Purkinje cell synapses (Foster et al., 2005), we found that AMPA receptors at parallel fiber–stellate cell synapses do not appear to be saturated, making this an unlikely explanation. Another possibility is that the changes in the postsynaptic calcium transient are below the signal-to-noise limit of this technique. Using paired-pulse stimulation, we found that the release probability on the second stimulus was ~325% of the first stimulus, while the calcium response of the second stimulus was ~180% of the first. Given that release probability in the presence of GABA was ~210% of control, and assuming a linear relationship between release probability and MVR, the predicted calcium response is only ~115% of control. This level of change may not be easily detected given the signal-to-noise ratio of these recordings, explaining the lack of observed change.

Antidromic propagation of subthreshold depolarizations

Several groups have recently shown that subthreshold somatic depolarizations can electrotonically spread out the axon several hundred micrometers (Alle and Geiger, 2006; Shu et al., 2006; Kole et al., 2007; Christie and Jahr, 2009). Basic cable properties of axons and recent experimental results predict that subthreshold depolarizations can also propagate in the antidromic direction (Scott et al., 2008; Paradiso and Wu, 2009; Trigo et al., 2010). In the present work, we show that $GABA_A$R-mediated depolarization of the axon can depolarize the soma. Subthreshold depolarizations may propagate antidromically with more efficiency in granule cell axons than other neuron types because they have only a single branch point and the somatodendritic compartments of these cells are relatively small. The diameter of the ascending axon is similar to that of the parallel fibers (0.1–0.2 μm) (Palay and Chan-Palay, 1974), creating relatively little impedance mismatch in the antidromic direction compared to that of small-diameter axon collaterals that branch off of much larger primary axons such as is observed in cortical pyramidal neurons. In fact, somatic depolarizations induced by GABA iontophoresis on axon collaterals of L5 pyramidal neurons are much smaller ($<$1 mV) (Christie and Jahr, 2009) than those observed in the present work (1–15 mV).

Paradiso and Wu (2009) have shown that subthreshold voltage changes in the calyx of Held can influence action potential initiation in the axon 400–800 μm away, but were not able to determine the effects on action potentials initiated at the axon initial segment. Trigo et al. (2010) recorded inward currents resulting from activation of axonal $GABA_A$Rs in somata of cerebellar stellate cells but did not assess the effects of these currents on excitability. We find that subthreshold depolarizations in the axon can promote initiation of orthodromic action potentials evoked by somatic depolarization. This suggests that subthreshold voltage changes initiated in the axon can be integrated with somatodendritic synaptic potentials to alter spike output of the neuron. In addition to the $GABA_A$R-mediated mechanism described here, subthreshold voltage changes can be elicited in the axon by other ligand-gated (Schmitz et al., 2001; Rusakov et al., 2005) and voltage-gated (Paradiso and Wu, 2009) channels. It is likely that subthreshold voltage changes produced by these mechanisms can also influence spike output of the neuron.

Functional implications

Spillover of GABA from neighboring synapses may have significant consequences on signal transfer and processing in the cerebellar cortex. Understanding the effects of GABA spillover is complicated by the fact that parallel fibers express both $GABA_A$ and $GABA_B$ receptors. While we have shown that $GABA_A$R activation increases calcium influx at parallel fiber varicosities and increases release at synapses onto MLIs, previous work has shown that $GABA_B$R activation has essentially opposite effects (Dittman and Regehr, 1997). However, rather than simply canceling one another out, the net effect of these two receptors may be to sharpen the timing of bursts in parallel fibers. $GABA_B$R-mediated effects on calcium influx and release do not peak until ~300 ms after receptor activation, whereas $GABA_A$R-mediated effects are nearly immediate. This leaves a window of ~200–300 ms in which synaptic transmission is enhanced by GABA spillover, after which transmission may return to baseline or be suppressed by $GABA_B$R activation.

$GABA_A$R activation during this window is likely to enhance the transmission of bursts of action potentials, a typical firing pattern seen in granule cells *in vivo* (Chadderton et al., 2004), but not of single spikes. Single action potentials in granule cells are poorly transmitted at parallel fiber synapses because of the low basal release probability (Dittman et al., 2000). Single action potentials are therefore unlikely to activate MLIs or presynaptic $GABA_A$Rs by spillover of GABA. However, bursts of action potentials are more reliably transmitted due to significant short-term facilitation at parallel fiber synapses (Konnerth et al., 1990; Perkel et al., 1990; Dittman et al., 2000) and enhanced release due to activation of presynaptic $GABA_A$Rs by GABA spillover. Furthermore, passive propagation of $GABA_A$R-mediated depolarization back to the soma increases excitability, possibly prolonging bursts. These mechanisms may help filter out postsynaptic effects of random, single spiking while enhancing the transmission and postsynaptic detection of bursts of spikes.

References

Alle H, Geiger JR (2007) GABAergic spill-over transmission onto hippocampal mossy fiber boutons. J Neurosci 27:942–950.

Alle H, Geiger JRP (2006) Combined analog and action potential coding in hippocampal mossy fibers. Science 311:1290–1293.

Awatramani GB, Price GD, Trussell LO (2005) Modulation of transmitter release by presynaptic resting potential and background calcium levels. Neuron 48:109–121.

Beierlein M, Gee KR, Martin VV, Regehr WG (2004) Presynaptic calcium measurements at physiological temperatures using a new class of dextran-conjugated indicators. J Neurophysiol 92:591–599.

Bender VA, Pugh JR, Jahr CE (2009) Presynaptically expressed long-term potentiation increases multivesicular release at parallel fiber synapses. J Neurosci 29:10974–10978.

Chadderton P, Margrie TW, Häusser M (2004) Integration of quanta in cerebellar granule cells during sensory processing. Nature 428:856–860.

Cherubini E, Gaiarsa JL, Ben-Ari Y (1991) GABA: an excitatory transmitter in early postnatal life. Trends Neurosci 14:515–519.

Christie JM, Jahr CE (2008) Dendritic NMDA receptors activate axonal calcium channels. Neuron 60:298–307.

Christie JM, Jahr CE (2009) Selective expression of ligand-gated ion channels in L5 pyramidal cell axons. J Neurosci 29:11441–11450.

Coombs JS, Curtis DR, Eccles JC (1957) The interpretation of spike potentials of motorneurons. J Physiol 139:198–231.

Dittman JS, Regehr WG (1997) Mechanism and kinetics of heterosynaptic depression at a cerebellar synapse. J Neurosci 17:9048–9059.
Dittman JS, Kreitzer AC, Regehr WG (2000) Interplay between facilitation, depression, and residual calcium at three presynaptic terminals. J Neurosci 20:1374–1385.
Dodt HU, Eder M, Schierloh A, Zieglgänsberger W (2002) Infrared-guided laser stimulation of neurons in brain slices. Sci STKE 2002:pl2.
Eccles JC, Schmidt R, Willis WD (1963) Pharmacological studies on presynaptic inhibition. J Physiol 168:500–530.
Ehrlich I, Lohrke S, Friauf E (1999) Shift from depolarizing to hyperpolarizing glycine action in rat auditory neurones is due to age-dependent Cl- regulation. J Physiol 520:121–137.
Flatman PW (2002) Regulation of Na-K-2Cl cotransport by phosphorylation and protein-protein interactions. Biochim Biophys Acta 1566:140–151.
Foster KA, Crowley JJ, Regehr WG (2005) The influence of multivesicular release and postsynaptic receptor saturation on transmission at granule cell to Purkinje cell synapses. J Neurosci 25:11655–11665.
Fuortes MGF, Frank K, Becker MC (1957) Steps in the production of motoneuron spikes. J Gen Physiol 40:735–752.
Goldberg JH, Tamas G, Aronov D, Yuste R (2003) Calcium microdomains in aspiny dendrites. Neuron 40:807–821.
Jang IS, Jeong HJ, Akaike N (2001) Contribution of the Na-K-Cl cotransporter on GABA(A) receptor-mediated presynaptic depolarization in excitatory nerve terminals. J Neurosci 21:5962–5972.
Jang IS, Ito Y, Akaike N (2005) Feed-forward facilitation of glutamate release by presynaptic GABA(A) receptors. Neuroscience 135:737–748.
Jang IS, Nakamura M, Ito Y, Akaike N (2006) Presynaptic GABAA receptors facilitate spontaneous glutamate release from presynaptic terminals on mechanically dissociated rat CA3 pyramidal neurons. Neuroscience 138:25–35.
Kanaka C, Ohno K, Okabe A, Kuriyama K, Itoh T, Fukuda A, Sato K (2001) The differential expression patterns of messenger RNAs encoding K-Cl cotransporters (KCC1,2) and Na-K-2Cl cotransporter (NKCC1) in the rat nervous system. Neuroscience 104:933–946.
Kandel ER, Spencer WA, Brinley FJ Jr (1961) Electrophysiology of hippocampal neurons. I. Sequential invasion and synaptic organization. J Neurophysiol 24:225–242.
Kelly L, Farrant M, Cull-Candy SG (2009) Synaptic mGluR activation drives plasticity of calcium-permeable AMPA receptors. Nat Neurosci 12:593–601.
Kocsis JD, Malenka RC, Waxman SG (1983) Effects of extracellular potassium concentration on the excitability of the parallel fibres of the rat cerebellum. J Physiol 334:225–244.
Kole MH, Letzkus JJ, Stuart GJ (2007) Axon initial segment Kv1 channels control axonal action potential waveform and synaptic efficacy. Neuron 55:633–647.
Konnerth A, Llano I, Armstrong CM (1990) Synaptic currents in cerebellar Purkinje cells. Proc Natl Acad Sci U S A 87:2662–2665.
Mikawa S, Wang C, Shu F, Wang T, Fukuda A, Sato K (2002) Developmental changes in KCC1, KCC2 and NKCC1 mRNAs in the rat cerebellum. Brain Res Dev Brain Res 136:93–100.
Nicoll RA, Alger BE (1979) Presynaptic inhibition: transmitter and ionic mechanisms. Int Rev Neurobiol 21:217–258.
Oertner TG, Sabatini BL, Nimchinsky EA, Svoboda K (2002) Facilitation at single synapses probed with optical quantal analysis. Nat Neurosci 5:657–664.
Palay SL, Chan-Palay V (1974) Cerebellar cortex: cytology and organization. New York: Springer.
Paradiso K, Wu LG (2009) Small voltage changes at nerve terminals travel up axons to affect action potential initiation. Nat Neurosci 12:541–543.
Perkel DJ, Hestrin S, Sah P, Nicoll RA (1990) Excitatory synaptic currents in Purkinje cells. Proc Biol Sci 241:116–121.
Pologruto TA, Sabatini BL, Svoboda K (2003) ScanImage: flexible software for operating laser scanning microscopes. Biomed Eng Online 2:13.
Pouzat C, Marty A (1999) Somatic recording of GABAergic autoreceptor current in cerebellar stellate and basket cells. J Neurosci 19:1675–1690.
Price GD, Trussell LO (2006) Estimate of the chloride concentration in a central glutamatergic terminal: a gramicidin perforated-patch study on the calyx of Held. J Neurosci 26:11432–11436.
Regehr WG, Tank DW (1991) Selective fura-2 loading of presynaptic terminals and nerve cell processes by local perfusion in mammalian brain slice. J Neurosci Methods 37:111–119.
Rinehart J, Maksimova YD, Tanis JE, Stone KL, Hodson CA, Zhang J, Risinger M, Pan W, Wu D, Colangelo CM, Forbush B, Joiner CH, Gulcicek EE, Gallagher PG, Lifton RP (2009) Sites of regulated phosphorylation that control K-Cl cotransporter activity. Cell 138:525–536.
Ruiz A, Fabian-Fine R, Scott R, Walker MC, Rusakov DA, Kullmann DM (2003) GABAA receptors at hippocampal mossy fibers. Neuron 39:961–973.
Ruiz A, Campanac E, Scott RS, Rusakov DA, Kullmann DM (2010) Presynaptic GABAA receptors enhance transmission and LTP induction at hippocampal mossy fiber synapses. Nat Neurosci 13:431–438.
Rusakov DA, Saitow F, Lehre KP, Konishi S (2005) Modulation of presynaptic Ca^{2+} entry by AMPA receptors at individual GABAergic synapses in the cerebellum. J Neurosci 25:4930–4940.
Schmitz D, Mellor J, Nicoll RA (2001) Presynaptic kainate receptor mediation of frequency facilitation at hippocampal mossy fiber synapses. Science 291:1972–1976.
Scobey RP, Gabor AJ (1975) Ectopic action-potential generation in epileptogenic cortex. J Neurophysiol 38:383–384.
Scott R, Ruiz A, Henneberger C, Kullmann DM, Rusakov DA (2008) Analog modulation of mossy fiber transmission is uncoupled from changes in presynaptic Ca^{2+}. J Neurosci 28:7765–7773.
Shu Y, Hasenstaub A, Duque A, Yu Y, McCormick DA (2006) Modulation of intracortical synaptic potentials by presynaptic somatic membrane potential. Nature 441:761–765.
Sipilä ST, Huttu K, Yamada J, Afzalov R, Voipio J, Blaesse P, Kaila K (2009) Compensatory enhancement of intrinsic spiking upon NKCC1 disruption in neonatal hippocampus. J Neurosci 29:6982–6988.
Soler-Llavina GJ, Sabatini BL (2006) Synapse-specific plasticity and compartmentalized signaling in cerebellar stellate cells. Nat Neurosci 9:798–806.
Stein V, Hermans-Borgmeyer I, Jentsch TJ, Hübner CA (2004) Expression of the KCl cotransporter KCC2 parallels neuronal maturation and the emergence of low intracellular chloride. J Comp Neurol 468:57–64.
Stell BM, Marty A (2009) Presynaptic GABA-A receptors modulate action potential induced calcium transients recorded in cerebellar parallel fibers. Soc Neurosci Abstr 35:416.16.
Stell BM, Rostaing P, Triller A, Marty A (2007) Activation of presynaptic GABA(A) receptors induces glutamate release from parallel fiber synapses. J Neurosci 27:9022–9031.
Szabadics J, Varga C, Molnár G, Oláh S, Barzó P, Tamás G (2006) Excitatory effect of GABAergic axo-axonic cells in cortical microcircuits. Science 311:233–235.
Trigo FF, Bouhours B, Rostaing P, Papageorgiou G, Corrie JE, Triller A, Ogden D, Marty A (2010) Presynaptic miniature GABAergic currents in developing interneurons. Neuron 66:235–247.
Turecek R, Trussell LO (2001) Presynaptic glycine receptors enhance transmitter release at a mammalian central synapse. Nature 411:587–590.
Turecek R, Trussell LO (2002) Reciprocal developmental regulation of presynaptic ionotropic receptors. Proc Natl Acad Sci U S A 99:13884–13889.
Xiao C, Zhou C, Li K, Ye JH (2007) Presynaptic GABAA receptors facilitate GABAergic transmission to dopaminergic neurons in the ventral tegmental area of young rats. J Physiol 580:731–743.
Yamada J, Okabe A, Toyoda H, Kilb W, Luhmann HJ, Fukuda A (2004) Cl^- uptake promoting depolarizing GABA actions in immature rat neocortical neurones is mediated by NKCC1. J Physiol 557:829–841.
Yuste R and Konnerth A, (2005) Imaging in neuroscience and development. Cold Spring Harbor, NY: Cold Spring Harbor Laboratory.
Zhang SJ, Jackson MB (1993) GABA-activated chloride channels in secretory nerve endings. Science 259:531–534.
Zhang SJ, Jackson MB (1995) GABAA receptor activation and the excitability of nerve terminals in the rat posterior pituitary. J Physiol 483:583–595.
Zhang W, Linden DJ (2009) Neuromodulation at single presynaptic boutons of cerebellar parallel fibers is determined by bouton size and basal action potential-evoked Ca transient amplitude. J Neurosci 29:15586–15594.